scientific reports

Check for updates

OPEN

Ultrasound guided blood brain barrier opening using a diagnostic probe in a whole brain model

Matteo Gionso[1,2], Erica Herlin[2,3], Laura Uva[4], Francesco Guidi[5], Piero Tortoli[5], Giovanni Durando[6], Luca Raspagliesi[1,2], Nicoletta Corradino[2,3], Veronica Percuoco[2,7], Francesco DiMeco[3,8,9], Marco De Curtis[4], Laura Librizzi[4] & Francesco Prada[2,8,10,11]✉

The blood–brain barrier (BBB) poses a significant challenge to drug delivery to the brain. A promising approach involves low-frequency, low-intensity pulsed ultrasound (US) waves combined with intravenously injected microbubbles (MB) to temporarily and non-invasively open the BBB. However, current technologies cannot easily integrate this procedure with US imaging. Passive cavitation detection, tracing the harmonic emissions of MB during sonication, has been the preferred method for real-time monitoring of US-mediated BBB opening. We used an ultrasound advanced open platform (ULA-OP) to simultaneously perform US-mediated BBB opening and US imaging with a single linear-array probe. In vitro guinea pig brains were perfused with MB and sonicated with different plane-wave transmission patterns. The most effective US pattern was interleaved with B-mode imaging pulses, enabling the direct assessment of the MB distribution during treatment. The extent of BBB permeabilization was assessed by quantifying FITC-albumin extravasation into the brain via confocal microscopy. US-treated hemispheres displayed BBB permeabilization, while control hemispheres did not. B-mode imaging allowed direct evaluation of MB distribution and interaction with the US beam. Therefore, we achieved effective BBB opening and simultaneous MB imaging using the same diagnostic probe, paving the way for US-guided therapeutic ultrasound application in the clinical context.

The blood–brain barrier (BBB) is a dynamic, semipermeable, and selective interface between cerebral vessels and the central nervous system (CNS). It is composed of endothelial cells, a basal membrane, mural cells, pericytes, and astrocytic glial cells, all of which work together to preserve the neural environment. Separating the circulating blood from the brain plays a critical role in controlling the influx and efflux of biological substances essential for brain function. However, the structural and molecular characteristics of the BBB significantly restrict successful drug delivery to the brain parenchyma, limiting the therapeutic effects of promising drug agents[1–3].

Several strategies have been proposed to overcome this barrier. In particular, the combined use of low-frequency, low-intensity ultrasound (US) waves and intravenously injected microbubbles (MB) has gained high interest, allowing a localized, reversible, and non-invasive opening of the BBB[4]. MB are ultrasound imaging contrast agents comprising encapsulated, gas-filled bubbles confined to the vasculature after intravenous injection due to their micrometer size[5]. US-induced BBB opening relies on the phenomenon of "acoustic cavitation", in which MB act as intravascular "cavitation nuclei", concentrating the acoustic energy within blood vessels and sparing surrounding neurons by reducing the required US intensity[6]. When driven by an intersecting US beam, MB oscillate at the same frequency as the applied US waves, a process known as stable cavitation, inducing shear stress on endothelial cells and loosening vessel wall junctions, temporarily increasing BBB permeability[7,8]. Increasing the acoustic pressure amplitude and the acoustic frequency results in larger

[1]Department of Biomedical Sciences, Humanitas University, Milan, Italy. [2]Acoustic Neuroimaging and Therapy Laboratory (ANTY-Lab), Fondazione IRCCS Istituto Neurologico "C. Besta", Via Celoria 11, 20133 Milan, Italy. [3]Department of Health Sciences, University of Milan, Milan, Italy. [4]Epilepsy Unit, Fondazione IRCCS Istituto Neurologico Carlo Besta, Milan, Italy. [5]Department of Information Engineering, University of Florence, Florence, Italy. [6]Ultrasound Laboratory, Istituto Nazionale di Ricerca Metrologica I.N.Ri.M., Turin, Italy. [7]Department of Neurosurgery, University Hospital Zurich, University of Zurich, Frauenklinikstrasse 10, 8091 Zurich, Switzerland. [8]Department of Neurological Surgery, Fondazione IRCCS Istituto Neurologico "C. Besta", Via Celoria 11, 20133 Milan, Italy. [9]Department of Neurological Surgery, Johns Hopkins Medical School, Baltimore, MD, USA. [10]Department of Neurological Surgery, University of Virginia Health System, Charlottesville, VA, USA. [11]Focused Ultrasound Foundation, Charlottesville, VA, USA. ✉email: francesco.prada@istituto-besta.it

MB oscillations and stronger microstreaming, shifting from stable non-inertial to inertial cavitation. This can result in adverse effects, such as shock waves and high-velocity jets, the release of free radicals, and high local temperatures[9,10]. Therefore, it is important to use sufficiently low-pressure amplitudes to avoid side effects while still inducing the desired BBB opening[9]. Contrast-enhanced MRI studies have shown that BBB opening can be achieved with acoustic pressure levels typically lower than 1 MPa, without detectable adverse effects[7,11]. The resulting temporary and reversible BBB impairment allows for greater drug delivery into the brain parenchyma within a restricted and controlled spatial and temporal window. After US-mediated BBB opening, endothelial cells show an increase in both transcellular and paracellular passages, as well as a higher number of vesicles, as identified by electron microscopy studies. These changes return to pre-treatment levels within approximately 4–6 h, confirming the temporary and reversible effects of US on the BBB[8,10].

Although transcranial US-induced BBB opening is a highly promising technique for treating CNS pathologies, current technologies are still facing limitations, particularly in real-time MB tracking during sonication procedures. Over the past decades, several techniques have been investigated for detecting and mapping MB. MRI and CT images, whether pre-acquired or obtained during sonication itself, can be confidently used for anatomical MB targeting and BBB opening with high spatial resolution[11–13]. However, imaging feedback is not possible with these techniques, as they cannot directly monitor the effect of cavitation. Consequently, efforts have been made to detect cavitation events using acoustic approaches to monitor US treatments by recording the emissions during transcranial focused ultrasound procedures. Acoustic detection methods, including active and passive cavitation detection techniques, rely on the acoustic emissions generated by cavitation bubbles[14]. In active cavitation detection (ACD), a US wave for imaging is transmitted, and echoes from cavitation bubbles are then imaged due to the difference in acoustic impedance between soft tissue and bubbles[15]. In passive cavitation detection (PCD), one or more receiver-only probes operate passively, without transmitting US waves, to transcranially acquire acoustic emissions stemming from the interaction between MB and brain tissue during BBB opening[14]. PCD is effective in monitoring cavitation events as well as providing information about the mode and strength of the oscillations in real-time, with studies linking cavitation activity to the degree of BBB opening[16–18]. Clinical trials on animal models have confirmed the efficacy of US-mediated BBB opening in combination with PCD[18,19]. Furthermore, Singh et al. (2022) recently described an all-US method for combining power Doppler imaging with a steerable focused ultrasound array to guide US-mediated BBB opening with high precision in rodents[20]. Three-dimensional passive cavitation detectors have also been used to monitor cavitation activity in three dimensions, ensuring precise targeting and minimizing off-target effects[21–23]. The efforts of these authors led to the development of passive acoustic mapping techniques, which exploit single or multiple passive cavitation detectors to spatially translate cavitation phenomena and to distinguish stable and inertial cavitation. These systems can monitor MB cavitation during sonication, allowing for MB spatial localization in the target area at a specific point in time. However, they cannot evaluate MB distribution before and after sonication, thus not allowing to study the distribution of MB in the 3D space over time. Furthermore, the acoustic feedback from PCD does not consider the real-time variations in the spatial accumulation or flow of intravascular MB among different brain regions and structures, which undoubtedly contributes to the bioeffects linked to BBB opening. Consequently, simultaneous US imaging could effectively evaluate the MB 3D distribution during repeated US-induced BBB opening procedures, enabling a tailored procedure and achieving the highest accuracy and precision of sonication protocols.

Contrast-enhanced US (CEUS) imaging is a proven tool for intraoperative MB distribution evaluation, enabling the assessment of brain perfusion in various regions, particularly when studying brain tumors. Different studies have highlighted the importance of intraoperative CEUS (iCEUS) imaging in brain tumor surgery[24–26]. The evaluation of intraoperative CEUS imaging is mainly qualitative, revealing differences in enhancing patterns when different structures are observed. However, Prada and colleagues (2021) also described the quantitative differences between different brain areas, as well as different grey and white matter regions[27]. Regarding treatment, identifying unique patterns of MB's distribution across different brain regions, including white and grey matter areas, could be beneficial to US-mediated BBB opening since different brain areas may display distinct BBB opening patterns due to variations in vascularity and, consequently, MB concentration. As a result, CEUS could be used to identify unique patterns of MB distribution, thereby enabling the detection of different patterns of BBB opening. In addition, by exploiting the intravascular cavitation of MB, it is possible to concentrate the mechanical effects of US waves into the vessels, while sparing the brain parenchyma. This autofocusing property of MB allows faster and more available treatments. Therefore, US-induced BBB opening might benefit from both an unfocused approach and CEUS-based planning and real-time feedback.

This study aimed to perform an effective US-guided BBB opening procedure by using a dual function – diagnostic and therapeutic – probe driven by a single ultrasound scanner. By using the ultrasound advanced open platform (ULA-OP) developed by the Microelectronics Systems Design Laboratory (MSD Lab) of the University of Florence, Italy, we conducted a BBB opening procedure in an in-vitro whole-brain preparation, shown to support brain sonication and real-time MB visualization without structural interference[28,29]. This approach focused on advanced ultrasound technology to achieve real-time monitoring and precise BBB opening.

Results

US-mediated BBB opening

Following the transmission of plane waves according to each of four therapeutic US (TUS) patterns (A, B, C, D), BBB opening was indirectly assessed by quantifying the fluorescent signal produced by FITC-albumin extravasation using confocal microscopy. The neocortex, hippocampal formation, and thalamus were analyzed, and the fluorescent signal resulting from each BBB opening procedure was precisely measured in each region. Control hemispheres were compared with brains treated with the different TUS patterns. For convenience, the most representative images were selected, resulting in twenty-five photomicrographs: twenty from treated

hemispheres, each specific to a sonication pattern and brain region, and five from selected regions in control brains. As illustrated in Fig. 1a, control hemispheres exhibited no BBB permeabilization, with very low fluorescent signal confined to the vasculature (first row in Fig. 1a). The most efficient BBB opening was observed when employing two specific sonication patterns, pattern A and pattern D. This was evidenced by the higher fluorescent signal observed around vessels and occupying almost the entire photomicrograph following the BBB opening procedure in each examined brain region (second and fifth rows in Fig. 1a). Conversely, brain sections subjected to patterns B and C exhibited a completely intraluminal signal, similar to controls, or at least a minimal

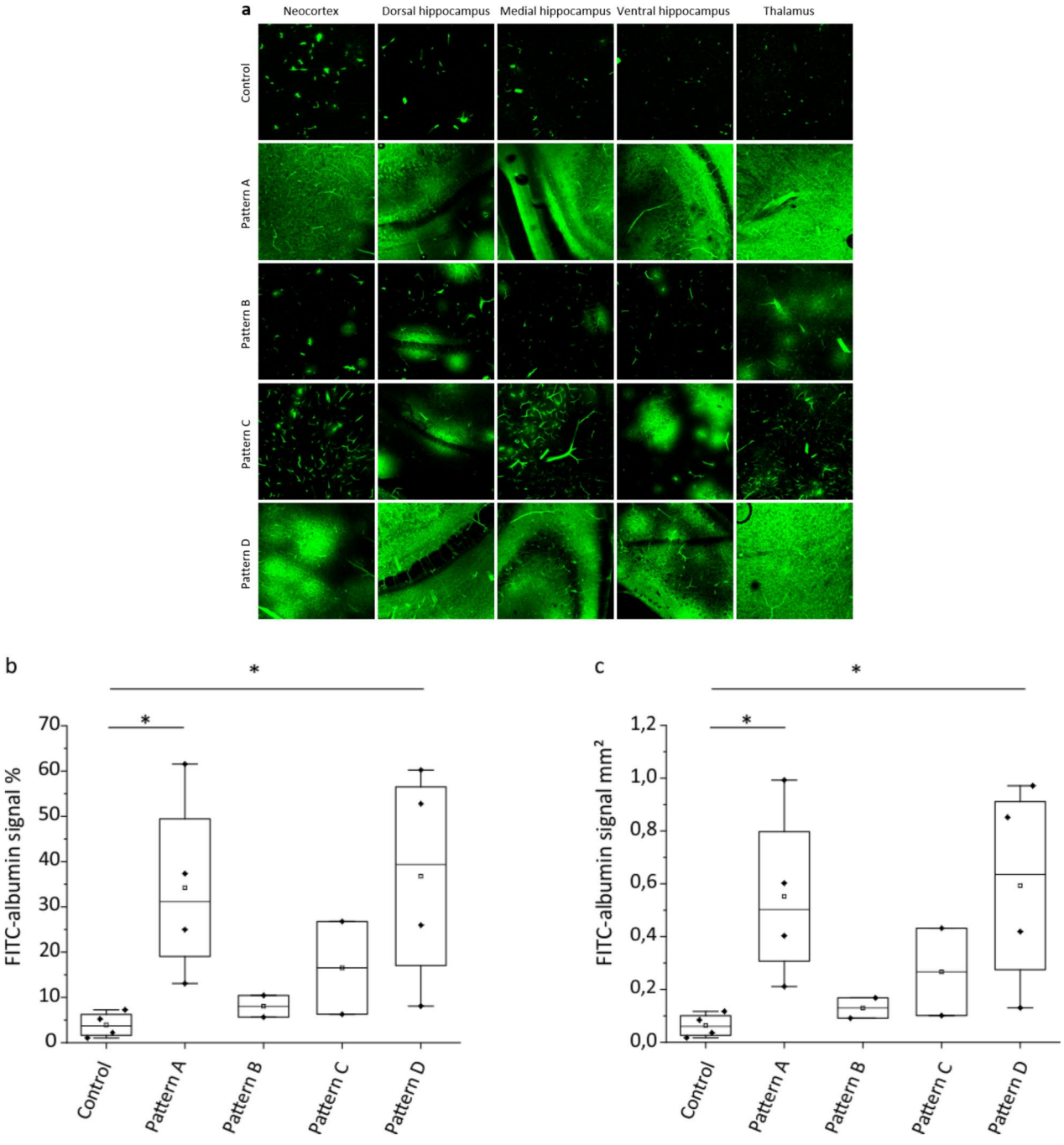

Fig. 1. (**a**) High-resolution confocal microscope photomicrographs of intra-parenchymal FITC-albumin signal in the neocortex, dorsal, medial, ventral hippocampus, and thalamus, following the application of the MB and different US sonication patterns. Control brains exhibited only intraluminal signal. Patterns B and C yielded predominantly intraluminal signal with dispersed perivascular spots. Pattern A and D resulted in more BBB opening, as evidenced by areas of FITC-albumin extravasation visible around the vessels. (**b**) and (**c**) Quantification of FITC-albumin was performed by measuring the area occupied by the fluorescent signal in the control hemispheres and across the four experimental conditions.

fluorescent signal around vessels (third and fourth rows in Fig. 1a). Across all regions analyzed, no significant qualitative differences in BBB opening were observed for individual sonication patterns. Quantification of the FITC-albumin signal through the Image-Pro Premier 9.1 software corroborated the confocal microscopy findings. Figure 1b,c present the average fluorescent signal values for each sonication pattern: Fig. 1b as percentage area and Fig. 1c relative to the 1.6 mm^2 ROI. Dots in both figures represent average values for each hemisphere across all five regions (neocortex, dorsal, ventral, medial hippocampus, and thalamus).

A significant increase in FITC-albumin signal was achieved through sonication patterns A (Fig. 1b,c; n = 4) and D (Fig. 1b,c; n = 4), respectively. In particular control vs pattern A (3.7 vs. 31.2% and 0.06 vs. 0.50 mm^2; U = − 2.1; $p \leq 0.05$). Control versus pattern D (3.7 vs. 394% and 0.06 vs. 0.63 mm^2; U = − 2,1; $p \leq 0.05$). In contrast, patterns B and C showed lower median values (8.03 and 16.5% and 0.12 and 0.26 mm^2, Fig. 1b,c; n = 2), respectively.

Real-time US imaging

Based on the results of the BBB opening procedure using the four sonication patterns, pattern D was selected. This pattern allowed the introduction of B-Mode imaging sequences between two consecutive treatment sequences, thereby enabling direct observation of the interaction between therapeutic US waves and previously infused MB. The novel pattern, including TUS and B-Mode pulses, is hereinafter called D3.

As shown in Fig. 2, the US probe was positioned in a coronal plane over the brain, with the therapeutic US beam intersecting solely the left hemisphere, while the diagnostic US beam intersected both hemispheres. Several frames were acquired during the BBB opening procedure, and a qualitative imaging analysis was performed throughout the treatment. Before starting the US treatment, real-time B-mode imaging permitted observing the movement and circulation of MB within both hemispheres (Fig. 2a; time t = 0″). The US treatment was initiated 48″ later. At t = 80″, just 32″ into the US treatment, a reduction in MB signal intensity was observed in the hemisphere corresponding to the US treatment area (Fig. 2b). The B-mode modality of the system showed a persistent reduction in MB signal even at the end of the US treatment, which occurred at t = 168″ (Fig. 2c). Finally, the restoration of the initial MB distribution was observed approximately at t = 180″ (Fig. 2d).

Discussion

In this study, we have demonstrated the feasibility of disrupting the BBB while concurrently performing B-mode imaging, through the use of a single clinical diagnostic probe.

The rationale behind this preclinical study was to investigate whether an open scanner, such as the ULA-OP system, could perform US imaging and therapeutic US treatments simultaneously. In recent studies, US-mediated BBB disruption has been assessed by different systems able to detect US emissions, but not through B-mode imaging performed by the same scanner used for treatment. Passive cavitation detection has been the preferred method for real-time monitoring of US-mediated BBB opening, tracing the harmonic emissions of MB during sonication[14]. However, PCD provides limited information, focusing only on the occurrence of cavitation, without evaluating MB distribution across time and space. Real-time CEUS imaging could overcome this limitation by assessing 3D MB distribution in target tissues during repeated therapeutic BBB procedures. This would allow tailored sonication parameters to minimize the impact on physiological structures.

Using the same scanner and the same probe to perform both US-mediated BBB-opening and CEUS imaging presents unavoidable technical challenges. These two modalities require the transmission of different US patterns. The imaging scanner used in this work was not designed to sustain transmission bursts several ms long, as usually requested in focused ultrasound approaches. Although this limitation could have been faced by modifying the electronics, we decided to exploit the system's flexibility to achieve the same overall sonication length through the transmission of multiple shorter bursts at relatively high PRFs. We could also test different transmission patterns and select the one most effective for BBB opening. Furthermore, this strategy permitted the switch between the transmission of therapeutic pulses, capable of creating large openings, and imaging pulses, although with a limited frame rate (4 Hz). Such a rate was sufficient to follow the phenomenon under investigation, but higher frame rates, if needed, could be achieved by fitting more imaging pulses (i.e. using higher PRF) between subsequent treatment pulses or even by applying high-frame rate US imaging methods[30].

An open scanner, such as the ULA-OP system, represents a preliminary step toward the development of fully US-based methods that can reliably modify sonication parameters in real-time, based on MB behavior in the target tissue. BBB opening was here achieved through the transmission of plane waves over the brain hemispheres after MB administration. By transmitting plane waves rather than focused waves, it was possible to sonicate a wide region for each transmission event[30]. Different increases in BBB permeability were observed by testing four different sonication patterns. As described in detail in the Methods section, these patterns were designed to generate transmission pulses with different durations and pulse repetition frequencies (PRFs). Patterns labeled A, B, and C were designed to sonicate with treatment pulses 2, 10, and 50 µs long at a PRF of 2000, 400, and 80 Hz, respectively, to maintain a duty cycle of 0.4%. A fourth model, labeled D, was designed to produce a sequence of 40 pulses, each 50 µs in duration, at a 2 kHz rate, followed by a pause of 480 ms. The increase in BBB permeability was then assessed by quantifying at confocal microscopy the extravasation of FITC-albumin perfused for 4 min at the end of each experiment. ULA-OP was effective in performing BBB opening in hemispheres exposed to concomitant sonication and MB administration. As shown in Fig. 1, patterns A and D were more effective than patterns B-C. This is due to the higher PRF (2 kHz) employed in A and D, which is needed to obtain adequate BBB-opening when working with low-pressure pulsed US (340 kPa). The most effective transmission pattern in terms of BBB opening (pattern D) was interleaved with the transmission of B-mode imaging sequences, leading to the creation of a new pattern, labeled pattern D3. This pattern was employed to observe the interaction between MB and TUS waves, which is the basis of BBB opening, and the effect that sonication has on MB distribution.

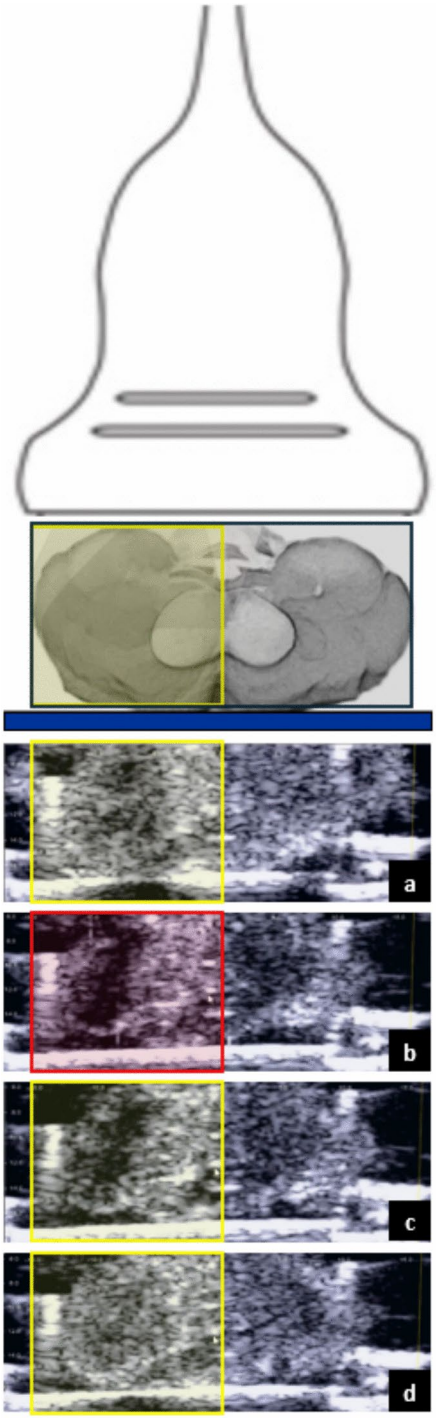

Fig. 2. B-mode images showing the MB distribution before (**a**), during (**b**,**c**), and after (**d**) the US-mediated BBB opening. The white line represents the base of support for the brain. The therapeutic US beam is targeted towards the left hemisphere, as indicated by the rectangles, while the grey diagnostic US beams intersect both hemispheres. The yellow color in the first, third, and fourth panels indicates that the TUS beam is off, whereas the red color in the second row indicates that the TUS beam is on. (**a**) B-mode acquisition before the start of US treatment, showing the MB distribution within the brain (time t = 0″). (**b**: t = 80″) and (**c**: t = 168″) Effects of the interfering TUS beam on MB distribution during and at the end of the US treatment, respectively. (**d**: t = 180″) B-mode acquisition following the conclusion of the US treatment.

During sonication, a reduction in MB signal intensity was observed in the treated area. This reduction can be attributed to the acoustic cavitation phenomenon. We believe that at least some MB collapse due to transient – not sustained—inertial cavitation caused by the pressures used by our ultrasound device. Being this effect only transient, the negative effects of sustained inertial cavitation were not observed in our model. This observation

is a crucial step to unveil MB dynamics during TUS procedures and was possible thanks to the concomitant US imaging provided by our system. The B-mode modality of the system demonstrated a persistent reduction in MB signals even after the US treatment. This probably indicates persistent cerebral hypoperfusion due to cerebral vasospasm, which persisted for approximately 12–15 s. The effect was only temporary, with the restoration of the initial MB distribution pattern, thereby confirming the reversibility of the BBB opening procedure. However, as sonication pattern D3 was used solely in the final experiment, further trials should be conducted with this pattern to verify the reproducibility of the results and to confirm the efficacy of B-mode imaging during BBB opening procedures.

This study provides evidence of the effectiveness of the ULA-OP system in real-time monitoring BBB opening, enabling both US imaging and US disruption treatment to be performed simultaneously. The anatomy of the brain and the circulation of MB were easily visualized through US imaging, and it was possible to observe real-time changes in the B-mode pattern during US treatment. This is of great relevance as it would allow us to adjust sonication parameters to align with the pattern of MB enhancement of target tissues. A significant aspect of this study is that the US probe was the same as those used in current clinical practice, possibly smoothening the transition between the pre-clinical and the clinical setting.

Unfortunately, the use of CEUS in neurosurgery is counteracted by the presence of the skull, which limits the use of real-time US imaging modality to in vitro settings or during in vivo surgery after the skull's removal. In this paper, we used the isolated guinea pig brain preparation, maintained in vitro by arterial perfusion, which retains normal physiological properties close to the in vivo condition and represents a unique experimental preparation in which neuronal connectivity between remote brain regions is completely preserved for several hours. Brain activity can be monitored by multisite extracellular, intracellular, and ion-selective neurophysiological recordings and by functional imaging[31,32]. The in vitro isolated guinea pig brain represents an optimal preparation for BBB opening procedures, as it provides a whole functioning brain with an intact BBB that can be sonicated and imaged without interfering structures. However, the use of the in vitro brain preparation also presents some limitations. Primarily, the in vitro nature of the study removes numerous potentially confounding factors that comprise a more complex in vivo model. The controlled brain delivery of MB and FITC-albumin is easily achieved in vitro, whereas it may be more difficult and unreliable when both compounds are delivered by intravenous perfusion in vivo. For a possible in vivo application, our group has proposed the use of sonolucent cranial prostheses, which were demonstrated to allow focal BBB opening under real-time imaging feedback in vitro[29]. Trans-prostheses BBB-opening would be performed post-operatively in a selected cohort of patients that require cranial surgery, such as patients harboring brain tumors. In this cohort, our approach does not increase the invasiveness of the standard of care and would allow us to follow-up patients with trans-prostheses US imaging and therapy in an out-patient setting.

The results of the present study represent a significant advance in the field of ultrasound-mediated BBB opening, overcoming the limitations of passive cavitation detectors. Our system exploits the ambivalent nature of MB, which can be used for both imaging and therapy, by using a single US probe capable of performing both TUS and imaging simultaneously. This approach allows for the direct assessment of MB circulation within the treated area, enabling real-time spatial imaging of TUS-induced BBB opening.

Materials and methods

Study design

16 hemispheres from 8 guinea pig brains were sonicated with the ULA-OP US system. For the first 7 brains, different TUS patterns, labeled from A to D, were programmed to understand which modality yields the best results in terms of BBB opening. In brain #8, one hemisphere was sonicated with a modified version of pattern D, designated as pattern D3, which includes imaging pulses, whereas the contralateral served as control.

The ULA-OP system

The ULA-OP system is an ultrasound advanced open platform designed, implemented, and tested by the MSD Lab (University of Florence, Italy)[28]. The ULA-OP platform consists of two boards that include all the electronics necessary to control (in groups of 64) up to 192 elements of an array probe. The ULA-OP system was designed to permit the testing of new and advanced US methods, including original beamforming strategies, real-time image processing, pulsed Doppler, and vector Doppler techniques[33].

The open scanner can be used with a wide range of US probes. In this project, it was coupled with the LA332 (Esaote SpA, Florence, Italy), a linear array of 144 elements operating in the frequency range of 3–11 MHz. The system was programmed to produce different US patterns (see Tables 1 and 2) addressed to induce the mechanical stimulation of the microbubbles. In all cases, 16 mm-wide plane waves were generated by 64 adjacent elements of the linear array probe through the transmission of 4 MHz sinusoidal pulses with programmable length (T) and pulse repetition frequency (PRF). The amplitude of these pulses produced a peak-negative-pressure (PNP) of 340 kPa in water. The total duration of the treatment interval was always 120″. T and PRF were set to obtain, altogether, approximately 0.5″ of sonication distributed over such an interval.

As reported in Table 2, the patterns labeled A, B, and C were designed to produce stimulation with PRF of 2 kHz, 400 Hz, and 80 Hz and correspondingly increasing pulse durations, so that a duty cycle (T × PRF) of 0.4% was maintained. The fourth pattern, labeled D, included a sequence of 40 pulses, each 50 µs long, at PRF = 2 kHz. After such a sequence, the transmission was paused for 480 ms, before being repeated until the 120 s treatment interval was fully covered. The pattern labeled D3 was derived from pattern D by inserting the transmission of B-Mode imaging sequences during the 480 ms of transmission pause. The imaging sequence, transmitting 144 pulses (3-cycle at 5 MHz), allowed to achieve an overall rate of 4 frames/s.

Brain	Hemisphere	Sonication pattern
1	1	Control
	2	A
2	3	Control
	4	D
3	5	Control
	6	A
4	7	A
	8	B
5	9	C
	10	D
6	11	D
	12	C
7	13	B
	14	A
8	15	D3
	16	Control

Table 1. Sonication patterns used for each brain hemisphere.

Pattern name	Treatment pulse duration (T) (μs)	PRF
A	2	2 kHz
B	10	400 Hz
C	50	80 Hz
D	50	2 kHz for 20 ms, followed by 480 ms of pause
D3	50	as D + B-Mode pulses (at 2 kHz PRF) transmitted during the 480 ms pause

Table 2. Main parameters of the transmission patterns used for BBB-disruption and B-Mode imaging.

The in vitro brain preparation

The experimental procedures and the animal care were conducted following the guidelines defined by the European Communities Council directive (2010/63/EU).), ARRIVE guidelines and RRR principles. Every effort was made to limit the number of animals used. The experimental protocol was reviewed and approved by the Ethics Committee and by the Committee on Animal Care and Use of the Fondazione IRCCS Istituto Neurologico *Carlo Besta* (Approval reference number: DO-01-2021).

According to the standard procedure described in previous literature, the brain is isolated from young adult female Hartley guinea pigs (150–200 g; Charles River, Calco, Italy)[31]. After isoflurane anesthesia (Aerrane, Baxter, 4%), the guinea pig is transcardially perfused using a peristaltic pump with a cold (15 °C) oxygenated (95% O_2 / 5% CO_2; pH 7.1) complex saline solution composed by NaCl, 126 mM, KCl, 3 mM, KH_2PO_4, 1.2 mM, $MgSO_4$, 1.3 mM, $CaCl_2$, 2.4 94 mM, $NaHCO_3$, 26 mM, glucose, 15 mM, 3% hydroxyethyl starch (Voluven, Fresenius Kabi) with M.W. of 130 KDa. Then, the animal is decapitated, and the brain is carefully transferred into the incubation chamber, whose bottom is coated with a US-absorbing plate. The brain's ventral surface is positioned upward to visualize the base of the brain, and the olfactory bulbs and the cervical spinal cord are held down by two silk threads for mechanical stabilization. After the dura mater's removal, a polyethylene cannula (terminal gauge 0.25 mm) is inserted into the basilar artery to allow the restoration of brain circulation with the above solution (pH 7.3) at a rate of 6 ml/min via a peristaltic pump (Gilson Minipulse 4). Then, the carotid and the hypophyseal arteries are closed to re-establish the physiological perfusion of the brain. The temperature of the incubation chamber is successively increased from 15 to 22 °C, with an increase of 0.2 °C per minute. Isolated in vitro guinea pig brain can maintain close to-physiological activity for approximately 6–8 h.

Microbubbles circulation and sonication protocol

MB (SonoVue, Bracco, Italy) infusion and US sonication protocols were conducted as in previous experiments[29]. MB were employed to obtain the necessary cavitating gas for US-mediated BBB opening. MB, provided as a sulfur hexafluoride powder, were dissolved in 10 ml of 0.9% NaCl solution (0.5–2.5 × 108 MB/ml). As shown in Fig. 3, MB were then perfused into the isolated guinea pig brain with a continuous infusion at a steady rate of 1 ml/min, through a syringe-infuser (KD Scientific) connected to the main arterial perfusion line. The BBB-opening sonication protocol started 1 min after MB infusion. At the end of sonication, the MB infusion was interrupted and a 5-min washout with standard solution followed. The LA332 probe was oriented in the coronal

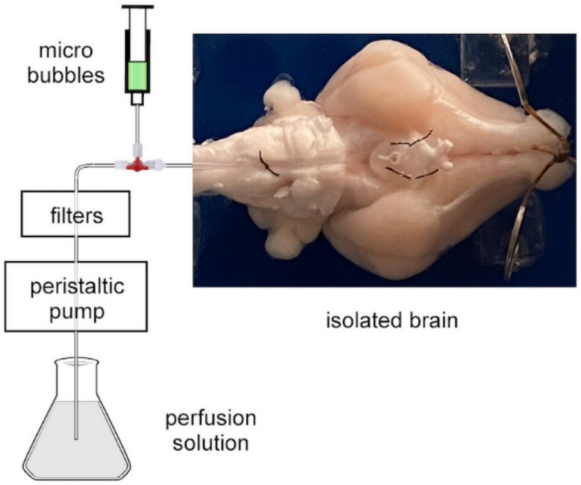

Fig. 3. Scheme of the experimental setup for MB perfusion via the resident arterial system of the in vitro isolated brain preparation. MB are injected via a syringe tributary of the main perfusion line.

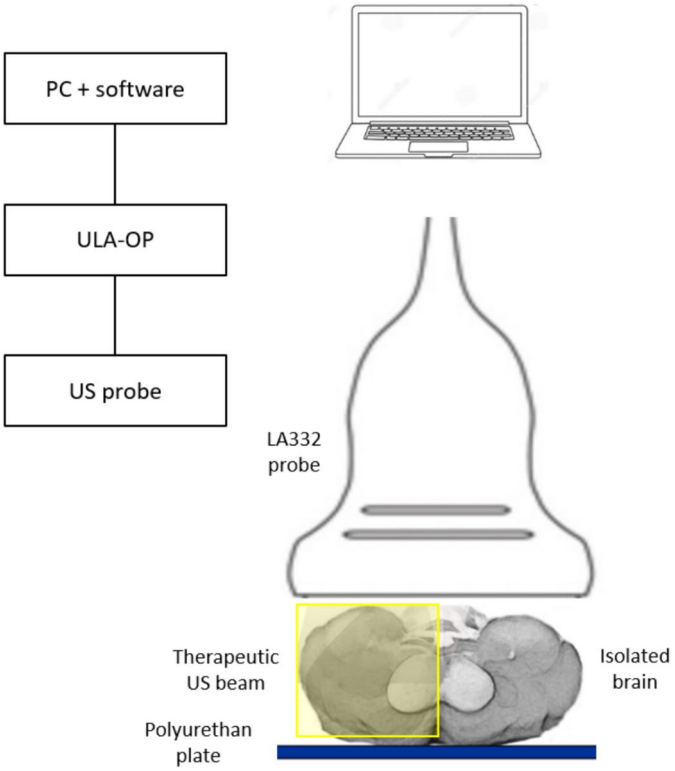

Fig. 4. Sonication set up. MB sonication was performed using the LA332 probe, connected to the ULA-OP platform and oriented in the coronal plane over the brain. The area of influence of the TUS beam was limited to one hemisphere. A US-absorbing polyurethane plate was positioned at the bottom of the incubation chamber to prevent US wave reflections.

plane over the brain, with the US beam directed to the target hemisphere, sparing the contralateral hemisphere (see Fig. 4). In the final experiment using the pattern D3, the same LA332 probe was used to achieve the BBB opening in the treated hemisphere and to visualize the MB in both the treated and untreated hemispheres.

Evaluation of BBB permeability change

The extravasation of fluorescein isothiocyanate (FITC)-albumin (50 mg/10 ml, Sigma – Aldrich), perfused for 4 min at the end of each experiment, was quantified using a confocal microscopy to evaluate US-mediated BBB opening. Brains were removed from the incubation chamber after each experiment and were fixed by immersion

for 48 h in a cold 4% paraformaldehyde solution in phosphate-buffered saline (PBS; 0.1 M, Ph 7.4). Serial coronal sections were obtained by vibratome (VT 1000S Leica) throughout the extension of the hippocampus (plates A5.4–A6.24 of the guinea pig brain atlas by Luparello); sections were then collected on gelatin-coated slides, mounted in Fluorosave (Calbiochem) and cover-slipped. Two representative sections corresponding to coronal rostral-caudal levels A5.40 and A6.00 of the Luparello atlas were collected for each brain. Slices were studied using a laser scanning confocal microscope D-Eclipse C1 (Nikon), equipped with three laser lines, mounted on a light microscope Eclipse TE2000-E (Nikon) using excitation light of 488 nm (Laser Ar). The FITC-albumin fluorescent signal was quantified in the neocortex, hippocampal formation, and thalamus. Five high-power non-overlapping fields (region of interest, [ROI] of 1.6 mm^2 each) per section were acquired bilaterally at × 10*g*, with an image size of 512 × 512 pixels. The Image-Pro Premier 9.1 software (Media Cybernetics) was used to assess and quantify the percentage of FITC-albumin signal (number of pixels) in each nonoverlapping field, and the data measured per slice were finally averaged, providing a single value for each hemisphere.

Statistical analysis

The normal distribution of samples was checked with the Shapiro-Wilks test and the homogeneity of variances was evaluated with the *F* test. The nonparametric Mann–Whitney tests was used. The format of Mann–Whitney test results is: median; U = x, $p \leq$ significance value. All statistical tests were performed with Origin 9.0 (OriginLab Corporation). The tests are two-sided and a confidence interval (CI) of 95% ($p \leq 0.05$) was required for values to be statistically significant. The data illustrated with boxplots show median (central line), quartiles (25% and 75%; box).

Data availability

The datasets used and/or analysed during the current study are available from the corresponding author on reasonable request.

Received: 3 December 2024; Accepted: 17 March 2025
Published online: 28 March 2025

References

1. Daneman, R. & Prat, A. The blood–brain barrier. *Cold Spring Harbor Perspect. Biol.* **7**(1), a020412. https://doi.org/10.1101/cshperspect.a020412 (2015).
2. Alahmari, A. Blood-brain barrier overview: Structural and functional correlation. *Neural Plast.* **2021**, 1–10. https://doi.org/10.1155/2021/6564585 (2021).
3. Kadry, H., Noorani, B. & Cucullo, L. A blood–brain barrier overview on structure, function, impairment, and biomarkers of integrity. *Fluids Barriers CNS* https://doi.org/10.1186/s12987-020-00230-3 (2020).
4. Deng, Z., Sheng, Z. & Yan, F. Ultrasound-induced blood-brain-barrier opening enhances anticancer efficacy in the treatment of glioblastoma: Current status and future prospects. *J. Oncol.* (2019).
5. Helfield, B. A review of phospholipid encapsulated ultrasound contrast agent microbubble physics. *Ultrasound Med. Biol.* **45**, 282–300. https://doi.org/10.1016/j.ultrasmedbio.2018.09.020 (2019).
6. Choi, J. J., Pernot, M., Small, S. A. & Konofagou, E. E. Noninvasive, transcranial and localized opening of the blood-brain barrier using focused ultrasound in mice. *Ultrasound Med. Biol.* **33**, 95–104 (2007).
7. Padilla, F., Brenner, J., Prada, F. & Klibanov, A. L. Theranostics in the vasculature: Bioeffects of ultrasound and microbubbles to induce vascular shutdown. *Theranostics* **13**(12), 4079–4101. https://doi.org/10.7150/thno.70372 (2023).
8. Burgess, A., Shah, K., Hough, O. & Hynynen, K. Focused ultrasound-mediated drug delivery through the blood–brain barrier. *Expert Rev. Neurother.* **15**(5), 477–491. https://doi.org/10.1586/14737175.2015.1028369 (2015).
9. Hosseinkhah, N. & Hynynen, K. A three-dimensional model of an ultrasound contrast agent gas bubble and its mechanical effects on microvessels. *Phys. Med. Biol.* **57**, 785–808 (2012).
10. Aryal, M., Arvanitis, C. D., Alexander, P. M. & McDannold, N. Ultrasound-mediated blood–brain barrier disruption for targeted drug delivery in the central nervous system. *Adv. Drug Deliv. Rev.* **72**, 94–109. https://doi.org/10.1016/j.addr.2014.01.008 (2014).
11. Carpentier, A. et al. Clinical trial of blood-brain barrier disruption by pulsed ultrasound. *Sci. Transl. Med.* https://doi.org/10.1126/scitranslmed.aaf6086 (2016).
12. Chen, K.-T. et al. Neuronavigation-guided focused ultrasound (NaviFUS) for transcranial blood-brain barrier opening in recurrent glioblastoma patients: Clinical trial protocol. *Ann. Transl. Med.* **8**, 673–673 (2020).
13. Mainprize, T. et al. Blood-brain barrier opening in primary brain tumors with non-invasive MR-guided focused ultrasound: A clinical safety and feasibility study. *Sci. Rep.* https://doi.org/10.1038/s41598-018-36340-0 (2019).
14. Izadifar, Z., Babyn, P. & Chapman, D. Ultrasound cavitation/microbubble detection and medical applications. *J. Med. Biol. Eng.* **39**(3), 259–276. https://doi.org/10.1007/s40846-018-0391-0 (2019).
15. Jeong, M. K., Choi, M. J. & Kwon, S. J. High-spatial-resolution, instantaneous passive cavitation imaging with temporal resolution in histotripsy: A simulation study. *Ultrasonography* **41**, 566–577 (2022).
16. Gyöngy, M. & Coussios, C.-C. Passive cavitation mapping for localization and tracking of bubble dynamics. *J. Acoust. Soc. Am.* **128**, EL175–EL180 (2010).
17. Haworth, K. J. et al. Passive imaging with pulsed ultrasound insonations. *J. Acoust. Soc. Am.* **132**, 544–553 (2012).
18. McDannold, N., Vykhodtseva, N. & Hynynen, K. Targeted disruption of the blood-brain barrier with focused ultrasound: Association with cavitation activity. *Phys. Med. Biol.* **51**, 793–807 (2006).
19. Morse, S. V. et al. Rapid short-pulse ultrasound delivers drugs uniformly across the murine blood-brain barrier with negligible disruption. *Radiology* **291**, 459–466 (2019).
20. Singh, A. et al. Guiding and monitoring focused ultrasound mediated blood–brain barrier opening in rats using power Doppler imaging and passive acoustic mapping. *Sci. Rep.* https://doi.org/10.1038/s41598-022-18328-z (2022).
21. Oreilly, M. A., Jones, R. M. & Hynynen, K. Three-dimensional transcranial ultrasound imaging of microbubble clouds using a sparse hemispherical array. *IEEE Trans. Biomed. Eng.* **61**, 1285–1294 (2014).
22. Jones, R. M. et al. Three-dimensional transcranial microbubble imaging for guiding volumetric ultrasound-mediated blood-brain barrier opening. *Theranostics* **8**, 2909–2926 (2018).
23. Hu, Z. et al. 3-D transcranial microbubble cavitation localization by four sensors. *IEEE Trans. Ultrason. Ferroelectr. Freq. Control* **68**, 3336–3346 (2021).
24. Prada, F. et al. Intraoperative contrast-enhanced ultrasound for brain tumor surgery. *Neurosurgery* **74**, 542–552 (2014).

25. Dixon, L., Lim, A., Grech-Sollars, M., Nandi, D. & Camp, S. Intraoperative ultrasound in brain tumor surgery: A review and implementation guide. *Neurosurg. Rev.* **45**(4), 2503–2515. https://doi.org/10.1007/s10143-022-01778-4 (2022).
26. Prada, F. et al. Multiparametric intraoperative ultrasound in oncological neurosurgery: A pictorial essay. *Front. Neurosci.* https://doi.org/10.3389/fnins.2022.881661 (2022).
27. Prada, F. et al. Quantitative analysis of in-vivo microbubble distribution in the human brain. *Sci. Rep.* https://doi.org/10.1038/s41598-021-91252-w (2021).
28. Tortoli, P. et al. ULA-OP: An advanced open platform for ultrasound research. *IEEE Trans. Ultrason. Ferroelectr. Freq. Control* **56**, 2207–2216 (2009).
29. Librizzi, L. et al. Ultrasounds induce blood–brain barrier opening across a sonolucent polyolefin plate in an in vitro isolated brain preparation. *Sci. Rep.* https://doi.org/10.1038/s41598-022-06791-7 (2022).
30. Tanter, M. & Fink, M. Ultrafast imaging in biomedical ultrasound. *IEEE Trans. Ultrason. Ferroelectr. Freq. Control* **61**, 102–119 (2014).
31. de Curtis, M., Librizzi, L. & Uva, L. The in vitro isolated whole guinea pig brain as a model to study epileptiform activity patterns. *J. Neurosci. Methods* **260**, 83–90. https://doi.org/10.1016/j.jneumeth.2015.03.026 (2016).
32. Librizzi, L., Janigro, D., De Biasi, S. & De Curtis, M. Blood-brain barrier preservation in the in vitro isolated guinea pig brain preparation. *J. Neurosci. Res.* **66**, 289–297 (2001).
33. Boni, E. et al. A reconfigurable and programmable FPGA-based system for nonstandard ultrasound methods. *IEEE Trans. Ultrason. Ferroelectr. Freq. Control* **59**, 1378–1385 (2011).

Acknowledgements

Part of the activities were granted through fellowships provided by the Focused Ultrasound Foundation, Charlottesville, VA, USA. We would like to thank the Ultrasound Lab of the Istituto Nazionale di Ricerca Metrologica (INRiM), Turin, Italy and the Department of Information [FP1] Engineering, University of Florence, Florence, Italy for sharing technical materials and advice.

Author contributions

F.P., P.T., F.G., M.D.C., L.L., L.U. designed and supervised the study and reviewed the manuscript; P.T. and F.G. provided ULA-OP system and parameters during all experiments; F.P., M.G., L.R., V.P., N.C. and G.D, performed insonations and ultrasonographic acquisitions, L.L., L.U. and E.H. provided the isolated brain preparations and the perfusion system and performed statistical analyses on BBB opening; L.L. and L.U. performed histological preparation of the specimens, acquired and analyzed the images at confocal microscopy; F.P., M.G., E.H., L.R., L.L., L.U. and F.G. manuscript drafting.

Declarations

Competing interests

The authors declare no competing interests.

Additional information

Correspondence and requests for materials should be addressed to F.P.

Reprints and permissions information is available at www.nature.com/reprints.

Publisher's note Springer Nature remains neutral with regard to jurisdictional claims in published maps and institutional affiliations.

Open Access This article is licensed under a Creative Commons Attribution-NonCommercial-NoDerivatives 4.0 International License, which permits any non-commercial use, sharing, distribution and reproduction in any medium or format, as long as you give appropriate credit to the original author(s) and the source, provide a link to the Creative Commons licence, and indicate if you modified the licensed material. You do not have permission under this licence to share adapted material derived from this article or parts of it. The images or other third party material in this article are included in the article's Creative Commons licence, unless indicated otherwise in a credit line to the material. If material is not included in the article's Creative Commons licence and your intended use is not permitted by statutory regulation or exceeds the permitted use, you will need to obtain permission directly from the copyright holder. To view a copy of this licence, visit http://creativecommons.org/licenses/by-nc-nd/4.0/.

© The Author(s) 2025